

# MODELLING SPACE WITH AN ATOM OF QUANTUM GEOMETRY

SETH A. MAJOR AND MICHAEL D. SEIFERT

ABSTRACT. Within the context of loop quantum gravity there are several operators which measure geometry quantities. This work examines two of these operators, volume and angle, to study quantum geometry at a single spin network vertex - “an atom of geometry.” Several aspects of the angle operator are examined in detail including minimum angles, level spacing, and the distribution of angles. The high spin limit of the volume operator is also studied for monochromatic vertices. The results show that demands of the correct scaling relations between area and volume and requirements of the expected behavior of angles in three dimensional flat space require high-valence vertices with total spins of approximately  $10^{20}$ .

## 1. INTRODUCTION

Several promising theories of quantum gravity predict that space is discrete. Within the context of loop quantum gravity, operators for area [1, 2, 3], volume [1, 4, 5], and possibly even angle [6] have discrete spectra. Given this radical departure from the paradigm of continuous space that has served us so well, it is important to study consequences of the suggested underlying discrete nature of space. This paper reports on a study on the angle and volume operators. More extensive discussion may be found in Ref. [7]. Some earlier results were reported in Ref. [8].

The eigenbasis for all geometric operators is the spin network basis. In this context spin networks are not merely a graphical notation for representation theory but also contain information that determines the properties of space. All geometric and matter degrees of freedom are contained in the network. Indeed, as traditional spin networks are embedded in a three dimensional space knots in the network contain physical information about the state of quantum geometry.

Geometric quantities are concentrated in the edges and vertices of the spin network. If an edge intersects a surface, the edge endows that surface with area. If a vertex (with valence larger than 3) is contained within a region, then the spin network vertex contributes volume to that region. The angle operator also is defined at a single spin network vertex. Since volume and angle are located at vertices, the spin network vertex may be called an “atom of geometry.” In addition if we look beyond the kinematic level, most of the current proposals to implement the Hamiltonian constraint contain operator expressions which act at the spin network vertex.

This work is a first step in what we call “single vertex studies.” Motivated by the fact that volume and angle operators act at a single vertex and the central importance of the spin network vertex in dynamics, we studied the relation on

---

*Date:* August 2001.

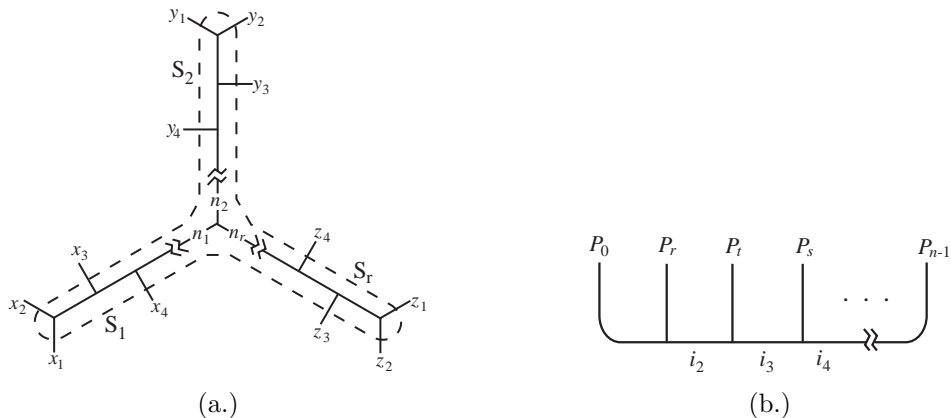


FIGURE 1. Two useful intertwiners. (a) Internal decomposition of a vertex operated on by the angle operator; the dotted line denotes the boundary between external and internal edges. All of the edges  $x_1, x_2, \dots$  which intersect the surface  $S_1$  are “collected” into the internal edge labelled with  $n_1$ ; similarly, all the edges which intersect  $S_2$  are collected into the edge labelled  $n_2$ , and the edges which intersect  $S_r$  are collected into the edge labelled  $n_r$ . In the text, we denote  $s_1 = \sum x_i$ ,  $s_2 = \sum y_i$ , and  $s_r = \sum z_i$ . This is called the snowflake basis. (b) The external edges  $P_0, P_1, \dots, P_{n-1}$  and the internal edges  $i_2, i_3, \dots, i_{n-2}$  of the comb basis.

the geometric quantities defined on this space. In such a simple context we can answer such questions as: “What are the properties of spin network states which approximate continuous space?” and, “What are some of the surprises that arise out of this new quantum geometry?”

In the next section we give the necessary notation, a very brief review of the angle operator, and the main analysis. In Section 3 we do the same for the volume operator. Section 4 contains a summary of the key points of the study and some additional consequences.

## 2. ANGLE RESULTS

Before reporting on the single vertex study of the angle and volume operators we need to introduce some notation on the spin network vertex. The number of incident edges is called the valence. While the internal structure of a trivalent vertex is unique, higher valence vertices can be constructed in more than one way. These different internal structures are described by the intertwiner, which labels the ways in which the incident representations are connected. Intertwiners therefore label a basis for the vertex.

The intertwiner may be described by a set of trivalent vertices connected by “internal edges.” When the edges are to be partitioned into three categories, as in the case of the angle operator, we can define a convenient basis in which the external edges of one category are collected in a branch which ends in one principal, internal edge. The three principal edges are then connected in a vertex we call the “intertwiner core.” This (class of) intertwiners is called the “snowflake” basis shown

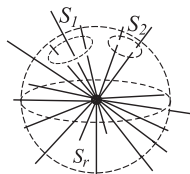


FIGURE 2. A vertex with three partitions of edges identified by the surfaces  $S_1$ ,  $S_2$ , and  $S_r$ . The core of the intertwiner for the vertex is chosen so that all edges passing through  $S_i$  connect to a single internal edge  $n_i$  (with  $i = 1, 2, r$ ) as shown in Figure 1a.

in Figure 1a. The core is the only part of the intertwiner which must be specified before completing the diagrammatic calculation of the angle spectrum. When all incident edges have the same label the vertex is called “monochromatic.”

**2.1. Angle operator: Definition.** The idea that one could measure angle from the discrete structure of spin networks was first suggested by Penrose [9]. This work culminated in the Spin Geometry Theorem, which stated that angles in 3-dimensional space could be approximated to arbitrary accuracy if the spin network was sufficiently correlated and if the spins were sufficiently large [10]. This result may be seen as the “high spin limit” of the observation that, for an EPR pair, we know the relative orientation of the particles’ spins but nothing about the absolute orientation of the two spins in a background space.

The spin geometry construction carries over into the context of quantum geometry: one can measure the angle between two internal edges of a spin network state. At the outset we note that there is more than one definition of the angle operator [6]. In this paper we use the quantization that most closely matches the operator in the spin geometry theorem. This angle operator is a quantization of the classical expression for an angle  $\theta_v$  measured at a point  $v$ . The operator assigns an angle to two bundles of edges incident to the vertex  $v$ . These edges are identified by the two surfaces  $S_1$  and  $S_2$  shown in Figure 2. Likewise, there are two angular momenta operators  $J_1$  and  $J_2$  associated to these surfaces. Acting on the spin network state  $|s\rangle$  the angle is [6]

$$\hat{\theta}_v^{(12)}|s\rangle := \arccos \frac{\hat{J}_1 \cdot \hat{J}_2}{|\hat{J}_1| |\hat{J}_2|} |s\rangle. \quad (1)$$

All edges incident to  $v$  are partitioned into three categories corresponding to which surface they pass through. In each category, the edges connect to a single internal edge in the intertwiner core. These edges are denoted  $n_1$ ,  $n_2$ , and  $n_r$ . For reasons that will be clear shortly, the spin  $n_r$  is known as the “geometric support.” Using the usual relations for angular momentum operators and an intertwiner core labelled by  $n_1$ ,  $n_2$  and  $n_r$ , one immediately finds the spectrum

$$\hat{\theta}_v^{(12)}|s\rangle = \arccos \left[ \frac{n_r(n_r + 2) - n_1(n_1 + 2) - n_2(n_2 + 2)}{2\sqrt{n_1(n_1 + 2)n_2(n_2 + 2)}} \right] |s\rangle. \quad (2)$$

We use the integer labels for which  $j_i = n_i/2$ . The key idea of the angle operator is to measure the relative spins of internal edges identified with the surfaces  $S_1$ ,  $S_2$ , and  $S_r$ .

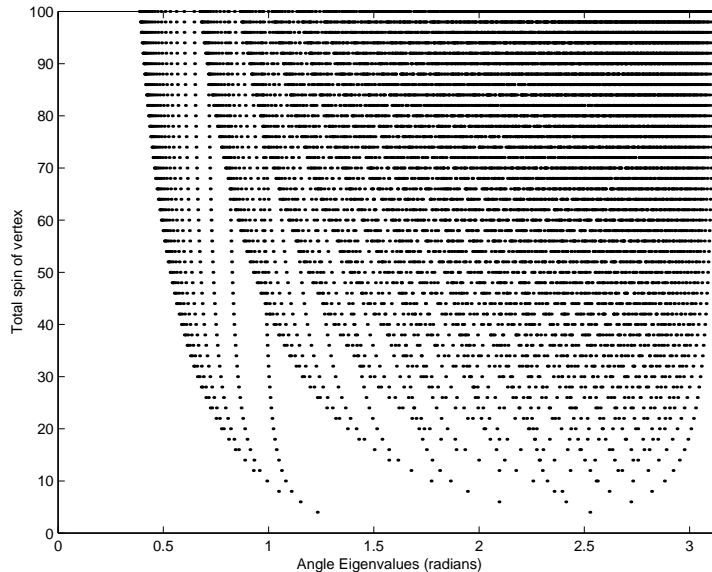


FIGURE 3. Angle operator spectrum for increasing total vertex spin  $n$ . The complete spectrum is plotted for total spins from 3 to 100.

Note that the quantities  $n_1$ ,  $n_2$ , and  $n_r$  are the internal edges that “collect” the spins from each of the three surface patches. They are related to the total edge flux intersecting each patch by the relations

$$n_1 \leq s_1, n_2 \leq s_2, \text{ and } n_r \leq s_r \quad (3)$$

where  $s_1$ ,  $s_2$ , and  $s_r$  are the respective surface fluxes.

Normally the discreteness in geometric observables such as area is on the Planck scale  $\ell_P \sim 10^{-35}$  m. However, angle operators have no dependence on the scale of the theory  $\ell_P$ . The result is *purely* combinatorial! This result provides a new test bed to investigate quantum geometry.<sup>1</sup>

Two aspects of the spectrum are immediately obvious from the spectra in Figure 3. First, the smallest angle can be quite large; it is “hard” to model small angles. Second, the gap between neighboring angles is non-uniform. It is clear from a glance that in order to model continuous space both of these effects must be minimized. In addition to these more obvious aspects, there is a requirement of these angles as embedded in three dimensional space on the distribution of angles. Each of these aspects are discussed in the following subsections.

<sup>1</sup>There is an important caveat: Retaining the diffeomorphism invariance of the classical theory in the construction of the state space, there is, generically, a set of continuous parameters or moduli space associated with higher valence vertices [11]. These parameters contain information on the embedding of the spin network graph in space. On such a space the angle spectrum is highly degenerate. It is by no means clear whether this embedding information is physically relevant [12]. Indeed, the state space of quantum gravity may be described by abstract or non-embedded graphs.

**2.2. Small Angles.** To obtain a small angle, we wish for the argument of the inverse cosine in (2),

$$Q \equiv \frac{n_r(n_r + 2) - n_1(n_1 + 2) - n_2(n_2 + 2)}{2\sqrt{n_1(n_1 + 2)n_2(n_2 + 2)}}, \quad (4)$$

to be as close to 1 as possible. However, the internal edge spins are subject to the triangle inequalities

$$2n_1, 2n_2, 2n_r \leq n_1 + n_2 + n_r.$$

To maximize  $Q$ , then, we wish to maximize its numerator and minimize its denominator while simultaneously respecting the triangle inequalities. This occurs when

$$n_r = \frac{n}{2} \text{ and } n_1 = n_2 \approx \frac{n}{4} \quad (5)$$

where the ‘‘spin sum’’  $n$  is defined as  $n = n_1 + n_2 + n_r$ .<sup>2</sup> At these values of  $n_1$ ,  $n_2$ , and  $n_r$ , the argument of the inverse cosine then reduces to

$$Q = \frac{n}{n + 8}. \quad (6)$$

For any angle  $\epsilon$ , then, we have the relation

$$\epsilon \geq \arccos\left(\frac{n}{n + 8}\right).$$

For small  $\epsilon$ ,  $\cos x$  is a uniformly decreasing function; hence, for  $\epsilon \ll 1$ , we have

$$\epsilon \geq \frac{4}{\sqrt{n + 8}}. \quad (7)$$

From this relation we see that the minimum possible angle between two patches is proportional to  $n^{-1/2}$  for large  $n$ . Moreover, we note that if  $s_r > s_1 + s_2$ , then  $n \leq 2(s_1 + s_2)$  which implies that for a ‘‘macroscopic’’ vertex, where  $s_r \gg s_1, s_2$ , the minimum observable angle depends only on the edge flux through the patches whose angular separation we are measuring. Since the total spin is bounded from above by twice the spin fluxes through the cones, the minimum observable angle depends on the area flux through the regions we are measuring. For instance, to achieve an angle as small as  $10^{-10}$  radians, the required flux is roughly  $10^{20}$ .

**2.3. Mean Angular Resolution.** The second property of the spectrum is the non-uniform level spacing. It is possible to quantify the angular resolution of a given vertex by counting the number of possible results of an angle measurement. We define the mean angular resolution  $\delta$  of a vertex to be the average separation between each possible angle and the next greatest possible angle. In other words,  $\delta$  is the average width of a ‘‘gap’’ between all possible angles in the interval  $[0, \pi]$ . This quantity is not the angular resolution for a given angle measurement; we do not compute the angle gap given an angle eigenvalue.

The simplest way of finding the mean angular resolution for a given vertex is to note that an  $n$ -valent vertex has  $n - 2$  trivalent vertices in its intertwiner. Since each one of these internal vertices can be looked at as a core vertex, we can conclude that such a vertex has at most  $3(n - 2)$  possible eigenvalues for the angle operator.

---

<sup>2</sup>Note that while the value for  $n_r$  is exact, the values of  $n_1$  and  $n_2$  are only approximate; this is because  $n$  must be even, but may not necessarily be divisible by 4, and because  $n_1$ ,  $n_2$ , and  $n_r$  must be integers. However, for large values of  $n$ , the values of  $n_1$  and  $n_2$  that maximize  $Q$  will approach  $n/4$ .

Since the  $3n-6$  eigenvalues associated with the vertex divide the interval into  $3n-5$  gaps, we conclude that the mean angular separation between the eigenvalues of the angle operator for an  $n$ -valent vertex is

$$\delta \geq \frac{\pi}{3n-5}.$$

The inequality accounts for possible degeneracies due to the fact that internal vertices may yield the same angles.

This method is limited. It only examines the separation between the eigenvalues of the angle operators that have a given vertex as their eigenstate. However, other angle measurements are possible for a given vertex. For example, if we measure the angle between two edges that do not immediately intersect in the vertex's intertwiner, this measurement will not always yield a definite eigenvalue. Instead, there will be an expectation value associated with this measurement. The question then becomes: for a given vertex, can we find the total number of possible expectation values?

To measure an angle we must partition the edges into three groups (one each for  $S_1, S_2,$  and  $S_r$ ). In the snowflake basis, we will generally obtain a superposition of angle eigenstates. Nonetheless, given a partition we will measure a single, definite expectation value, despite the superposition of eigenvalues. We conclude that the number of possible expectation values is equal to the number of distinct partitions of the edges.

Since the possible range of colours for the collecting edge is not dependent on the order of the edges along the branch, the number of distinct partitions is given by

$$\mathcal{N} = \prod_{i=1}^{\infty} B(q_i), \quad (8)$$

where  $q_i$  is the number of edges with colour  $i$ , and  $B(n)$  is the number of distinct ways of partitioning  $n$  into three distinct bins. Elementary combinatorics tells us that the number of ways to do this is

$$B(n) = \binom{(n+3)-1}{n} = \frac{(n+1)(n+2)}{2}. \quad (9)$$

We must divide the overall product by two, since exchange of the sets corresponding to the  $n_1$  branch and the  $n_2$  branch yields the same angle. Thus, the maximum number of possible expectation values for a given vertex is

$$\mathcal{N} = \frac{1}{2} \prod_{i=1}^{\infty} \frac{(q_i+1)(q_i+2)}{2}. \quad (10)$$

In the monochromatic case, where all the edges have the same colour,  $q_i$  is equal to the vertex valence  $n$  for one value of  $i$  (the edge colour) and zero otherwise. The formula reduces to

$$\mathcal{N} = \frac{(n+1)(n+2)}{4} \quad (11)$$

and the mean angular resolution (between expectation values) is given by

$$\delta_v \geq \frac{4\pi}{n^2 + 3n + 3} \quad (12)$$

where we have again used an inequality because of possible angle degeneracies.

It is important not to confuse the “mean angular resolution” as we have defined it with the average distance from a random point in the interval  $[0, \pi]$  to the nearest angle. What we have found allows us to get an idea of how tightly, on average, the eigenvalues of the angle operator for a given vertex are spaced. To find this other value (which, if found, would help us to estimate the level to which an arbitrary angle can be approximated) we would need

$$\langle \Delta \rangle = \sum_{\text{all gaps}} \left( \begin{array}{c} \text{prob. of being} \\ \text{located in the gap} \end{array} \right) \left( \begin{array}{c} \text{mean separation from} \\ \text{either end of gap} \end{array} \right). \quad (13)$$

This is equivalent to the expression

$$\langle \Delta \rangle = \sum_a \frac{w_a^2}{4\pi} \quad (14)$$

where  $w_a$  is the width of the gap  $a$ . This expression depends heavily on the precise location of the eigenvalues in the interval  $[0, \pi]$ , and is therefore difficult to compute analytically.

**2.4. Angle Distribution.** In the classical continuum model of 3-dimensional space, the distribution of solid angles is proportional to  $\sin \theta$

$$\mathcal{P}(\theta) d\theta = \sin \theta d\theta. \quad (15)$$

If our quantized angle operator is to be viable, it must reproduce this distribution in some “classical limit.” To find out whether this is so, we must examine not only the location of possible eigenvalues in the interval  $[0, \pi]$ , as we have in the past two subsections, but also the likelihood with which these angles occur. Due to the complexity of this problem, we will consider only the simplest possible case which could still conceivably have a classical limit: that of an  $n$ -valent monochromatic vertex with edge colour 1.

We note that every vertex can be transformed into the snowflake basis by repeated application of the recoupling theorem. For a random vertex, however, we do not know the exact internal structure *a priori*; there is no reason to assume that any given intertwiner is preferred. We will therefore assume that all intertwiners are equally likely. With this simplification in mind, we can conclude that the probability of measuring the angle associated with an intertwiner core  $n_1, n_2, n_r$  is given by

$$\mathcal{P}(\theta(n_1, n_2, n_r)) \propto \left( \begin{array}{c} \text{number of intertwiners} \\ \text{with core } n_1, n_2, n_r \end{array} \right). \quad (16)$$

We wish to know, then, how many intertwiners exist with a given  $n_1, n_2$ , and  $n_r$ . It can be shown that if  $i$  is the number of edges (of colour 1) entering a branch, the number of distinct branches  $\{a_2, a_3, \dots, a_i\}$  that end in a given  $n_1 = a_i$  is [7]

$$Q(i, a_i) = \frac{i+1}{a_i+1} \binom{a_i+1}{\frac{a_i+i}{2}+1} \quad (17)$$

To turn this into a normalized probability distribution, we approximate the binomial coefficient in the above expression by a Gaussian distribution multiplied by a normalization factor

$$\binom{x}{y} = A \exp \left[ \frac{-(x - \frac{y}{2})^2}{\frac{y}{2}} \right],$$



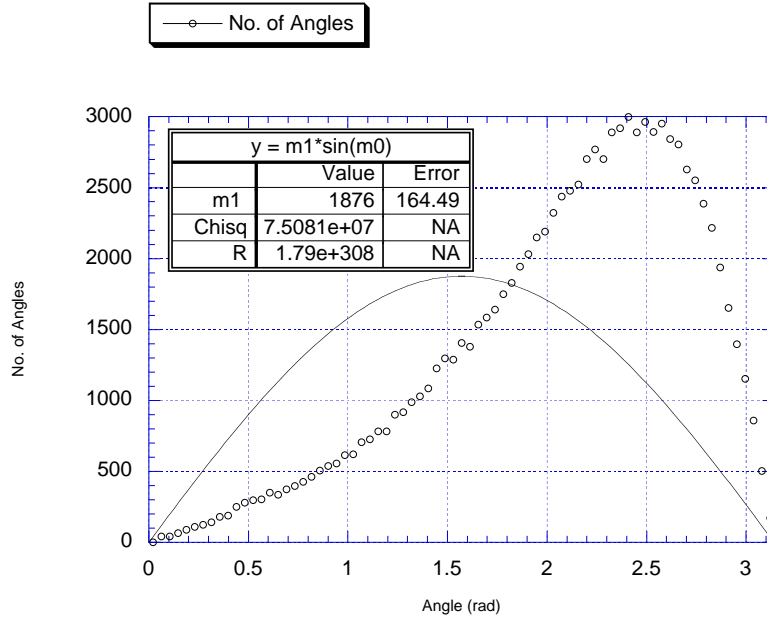


FIGURE 4. Angle distribution for  $s_1 = s_2 = s_r$ .

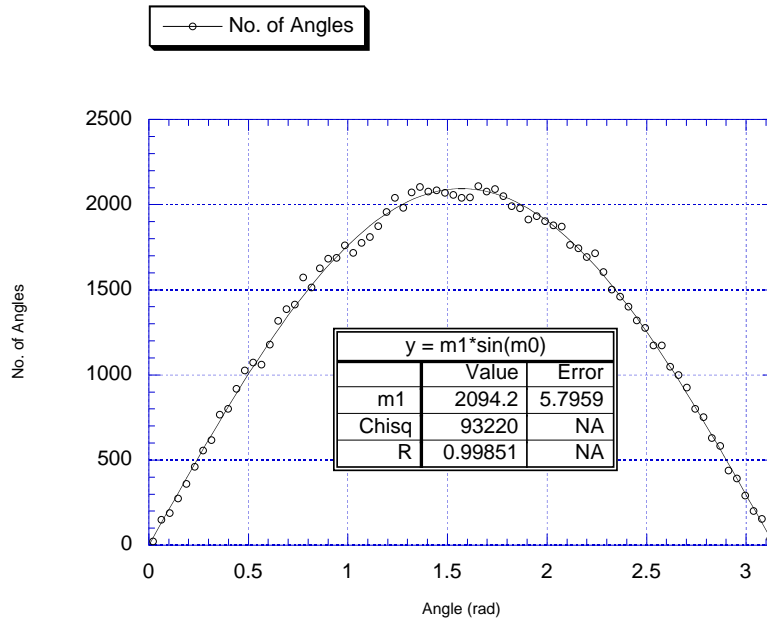


FIGURE 5. Angle distribution for  $s_1 < s_2 \ll s_r$ .

We can write the left hand side of this equation as a superposition of other vertices with the same internal decomposition as those in Figure 1b

$$\hat{W}_{[rst]} \left( \begin{array}{c} P_0 \quad P_r \quad P_t \quad P_s \quad \dots \quad P_{n-1} \\ \left| \quad \left| \quad \left| \quad \left| \quad \left| \quad \left| \right. \right. \right. \\ \left| \quad \left| \quad \left| \quad \left| \quad \left| \quad \left| \right. \right. \right. \\ i_2 \quad i_3 \quad i_4 \quad \dots \quad \dots \end{array} \right) = \sum_{k_2, \dots, k_{n-2}} W_{[rst]}^{k_2, \dots, k_{n-2}} \left( \begin{array}{c} P_0 \quad P_r \quad P_t \quad P_s \quad \dots \quad P_{n-1} \\ \left| \quad \left| \quad \left| \quad \left| \quad \left| \quad \left| \right. \right. \right. \\ \left| \quad \left| \quad \left| \quad \left| \quad \left| \quad \left| \right. \right. \right. \\ k_2 \quad k_3 \quad k_4 \quad \dots \quad \dots \end{array} \right) . \quad (20)$$

This is essentially a matrix equation with the entries of the matrix indexed by the internal intertwiner edges. These entries turn out to be [5]

$$W_{[rst]}^{(n) k_2 \dots k_{n-2}} = -P_r P_s P_t \left\{ \begin{array}{c} k_2 \quad P_t \quad k_3 \\ i_2 \quad P_t \quad i_3 \\ 2 \quad 2 \quad 2 \end{array} \right\} \lambda_{k_2}^{i_2} \delta_{i_4}^{k_4} \dots \delta_{i_{n-2}}^{k_{n-2}} \\ \times \frac{\left\{ \begin{array}{c} P_r \quad P_r \quad P_0 \\ k_2 \quad i_2 \quad 2 \end{array} \right\} \left\{ \begin{array}{c} P_s \quad P_s \quad k_4 \\ k_3 \quad i_3 \quad 2 \end{array} \right\}}{\theta(k_2, k_3, P_t)}. \quad (21)$$

In this formula we have used the 9- $j$  symbol, which is equivalent to the spin network

$$\left\{ \begin{array}{c} k_2 \quad P_t \quad k_3 \\ i_2 \quad P_t \quad i_3 \\ 2 \quad 2 \quad 2 \end{array} \right\} = \begin{array}{c} \begin{array}{c} k_2 \quad k_3 \\ \left| \quad \left| \right. \\ \left| \quad \left| \right. \\ i_2 \quad 2 \quad P_t \quad i_3 \\ \left| \quad \left| \right. \\ \left| \quad \left| \right. \\ 2 \end{array} \end{array} \end{array} \quad (22)$$

The eigenvalues of the volume-squared operator are then proportional to the sum of the absolute values of the eigenvalues of the  $W$ -operators

$$V^2 = \sum_{0 \leq r < s < t \leq n-1} \left| \frac{i}{16} W_{[rst]} \right|, \quad (23)$$

and the volume eigenvalues are the square roots of the eigenvalues of the  $V^2$  operator.

**3.2. The  $W$ -matrix and Eigenvalue Bounds.** One can see that the expression for the volume of Eq. (23) is horrendously difficult to handle in all its generality, for three main reasons. First, for an  $n$ -valent vertex with arbitrary edge colours, there are  $\binom{n}{3}$  possible choices for  $r$ ,  $s$ , and  $t$ ; each of these choices could conceivably produce a different  $W_{[rst]}^{(n)}$ . Second, the eigenvalues of the  $\hat{V}^2$  operator are difficult to find; even those of the  $W$ -matrix are distinctly non-trivial, since all that Eq. (21) gives us is the matrix entries. Third, the matrix entries themselves, as given by Eq. (21), are not easy to calculate analytically.

With these problems, it is to our advantage to make some simplifications. Instead of considering an arbitrary vertex, we will examine the case of a monochromatic vertex for which all of the matrices  $W_{[rst]}^{(n)}$  are identical (since our “graspings” are always on edges of the same colour).<sup>3</sup> The formula for volume reduces to

$$\hat{V}^2 = \binom{n}{3} \left| \frac{iW^{(n)}}{16} \right| = \frac{n(n-1)(n-2)}{96} |iW^{(n)}| \quad (24)$$

<sup>3</sup>In this case, we will often suppress the indices  $[rst]$ , since they are always the same; in other words, when referring to the monochromatic case, we will define  $W^{(n)} = W_{[rst]}^{(n)}$ .

This solves our first problem. The second problem, however, is somewhat less tractable. The matrix  $W^{(n)}$  has a row for each possible intertwiner core - usually a fairly large number. To get around this, we will examine bounds on the eigenvalues instead of the eigenvalues themselves. For any  $n \times n$  matrix with entries  $a_{ij}$ , any given eigenvalue  $\lambda$  of this matrix satisfies

$$|\lambda| \leq \max_i \sum_{j=1}^n |a_{ij}| \quad \text{and} \quad |\lambda| \leq \max_j \sum_{i=1}^n |a_{ij}|. \quad (25)$$

In other words, the magnitude of every eigenvalue must be less than the sum of the absolute values of some column and of some row. Using this, we can find an upper bound  $M$  on the magnitudes of the eigenvalues of  $W^{(n)}$ . In the monochromatic case the eigenvalues  $\lambda_{W_\alpha}$  of the  $\hat{W}^{(n)}$  operator are related to the eigenvalues  $\lambda_{V^2_\alpha}$  of the  $\hat{V}^2$  operator by

$$\lambda_{V^2_\alpha} = \frac{n(n-1)(n-2)}{96} |\lambda_{W_\alpha}| \quad (26)$$

as can be seen from (24). Hence, we can place a limit on the eigenvalues of the volume operator,  $\lambda_{V_\alpha} = \sqrt{\lambda_{V^2_\alpha}}$ ,

$$\lambda_{V_\alpha} \leq \sqrt{\frac{n(n-1)(n-2)}{96}} M. \quad (27)$$

The determination of the upper bound  $M$  is also rather complex. Simpler expressions do exist for the case of a 4-valent vertex; in this case, we can easily calculate the matrix elements explicitly. For higher valence vertices, numerical techniques come in handy.

**3.3. Volume Eigenvalue Bounds for 4-valent Vertices.** In the case of a 4-valent vertex, De Pietri [13] has shown that the entries of the  $W^{(4)}$  matrix for a 4-valent vertex with edge colours  $a, b, c$ , and  $d$  are given explicitly by the formula

$$\begin{aligned} W_{[012]^{t-\epsilon}}^{(4) \ t+\epsilon} &= \frac{-\epsilon(-1)^{(a+b+c+d)/2}}{32\sqrt{t(t+2)}} \\ &\quad [(a+b+t+3)(c+d+t+3)(1+a+b-t) \\ &\quad (1+c+d-t)(1+a+t-b)(1+b+t-a) \\ &\quad (1+c+t-d)(1+d+t-c)]^{\frac{1}{2}}. \end{aligned} \quad (28)$$

where  $t+\epsilon$  and  $t-\epsilon$  correspond to the internal edge of the vertex. It can be shown that these elements are zero unless  $\epsilon = \pm 1$ ; thus, each row or column will have at most two non-zero elements. To find  $M$  in this case all we have to do is to find the maximum value of this polynomial.

In the monochromatic case,  $a = b = c = d$ ; we call this edge colour  $m$ . The polynomial in question becomes

$$\left| W_{[012]^{t-\epsilon}}^{(4) \ t+\epsilon} \right| = \frac{(2m+t+3)(2m-t+1)(t+1)^2}{32\sqrt{t(t+2)}}. \quad (29)$$

Thinking of  $W$  as a continuous function  $W(t)$ , this expression is maximized at

$$t_{max} = -1 + \sqrt{\frac{(2m+2)^2 + 4}{6} + \frac{1}{6}\sqrt{(2m+2)^4 - 16(2m+2)^2 + 16}}, \quad (30)$$

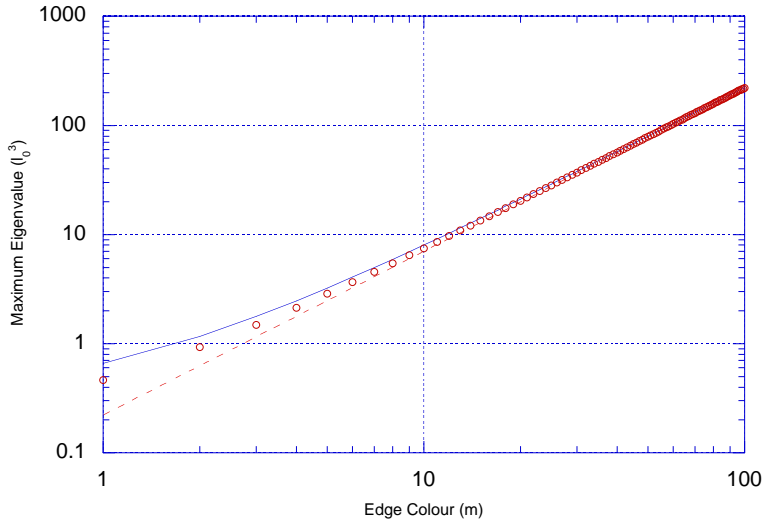


FIGURE 6. The eigenvalue limit obtained in (29) and (30), compared with the maximum volume eigenvalue for  $1 \leq m \leq 100$ . The lower dotted line is the result of a curve fit of the maximum eigenvalues to a curve of the form  $\lambda = km^{3/2}$ , where  $k$  is the only free parameter of the fit. This fit yields a value of  $k = 0.22155$ .

and the maximum value is, of course,  $W(t_{max})$ . In the large-spin limit, where  $m \gg 1$ , this maximum value scales as

$$|W_{max}| \approx \frac{m^3}{6\sqrt{3}}. \quad (31)$$

The maximum absolute row or column sum (i.e. the quantity  $M$ ) is at most twice this number; therefore, (27) tells us that for a 4-valent monochromatic vertex with edge colour  $m$ , any eigenvalue  $\lambda_V$  of the volume operator on this vertex will satisfy (more or less) the inequality

$$\lambda_V \leq l_V^3 \frac{m^{3/2}}{\sqrt{12\sqrt{3}}}. \quad (32)$$

This is a very encouraging result when we consider it in relation to the area operator. The eigenvalues of the area operator are given by [1, 2, 3]

$$\lambda_A = \ell_P^2 \sum_i \sqrt{m_i(m_i + 2)} \quad (33)$$

where the values  $m_i$  are all the intersections of edges with the surface in question. For a 4-valent vertex with large edge colour  $m$ , we have

$$\lambda_A \propto m. \quad (34)$$

Together with (32), this implies that the volume scales no faster than  $A^{3/2}$ , which is what we would expect from classical spatial geometry.

We must ask ourselves, however, how “good” this bound is: do the eigenvalues actually scale proportionally to  $m^{3/2}$ , and if so, is the proportionality coefficient

we have found (i.e.  $1/\sqrt{12\sqrt{3}}$ ) close to the actual proportionality coefficient? Figure 6 shows the largest eigenvalue of the volume operator (found by numerical calculation) compared to the bound stated in (29) and (30). As we can see, the bound fits the volume eigenvalues very tightly, diverging significantly from them for  $n < 10$  and becoming practically indistinguishable from the maximum eigenvalue for  $n > 50$ .

**3.4. Eigenvalue Bounds for  $n$ -Valent Vertices.** We now turn our attention to the more general case of the  $n$ -valent monochromatic vertex. In this case, we cannot use the simple formula of the four-valent case, but must instead use the more general form. There are some simplifications that can be made which aid us in computing these matrix entries and their bounds. Numerical methods prove to be fruitful.

We recall that we are examining the special case where  $P_r = P_s = P_t = P_0 = m$ . We note that the expression for the 9- $j$  symbol in Eq. (21) is fairly symmetric, and can be simplified. This symbol corresponds to the spin network

$$\left\{ \begin{array}{ccc} k_2 & P_t & k_3 \\ i_2 & P_t & i_3 \\ 2 & 2 & 2 \end{array} \right\} = \text{Diagram} \quad (35)$$

Using usual recoupling moves we can move the graspings of the 2-edges and close the resulting ‘‘triangles’’ to obtain

$$\left\{ \begin{array}{ccc} k_2 & m & k_3 \\ i_2 & m & i_3 \\ 2 & 2 & 2 \end{array} \right\} = \frac{\lambda_{k_3}^{i_3 2}}{m} \left( \frac{-i_2 \text{Tet} \begin{bmatrix} k_2 & i_2 & i_2 \\ 2 & 2 & 2 \end{bmatrix}}{\theta(k_2, i_2, 2)} + \frac{i_3 \text{Tet} \begin{bmatrix} k_3 & i_3 & i_3 \\ 2 & 2 & 2 \end{bmatrix}}{\theta(k_3, i_3, 2)} \right) \text{Tet} \begin{bmatrix} k_2 & k_3 & 2 \\ i_3 & i_2 & m \end{bmatrix}.$$

Plugging this back in, (21) becomes

$$W_{[rst]i_2 \dots i_{n-2}}^{(n) k_2 \dots k_{n-2}} = -m^3 \mathcal{Q} \lambda_{k_2}^{i_2 2} \delta_{i_4}^{k_4} \dots \delta_{i_{n-2}}^{k_{n-2}} \times \frac{\text{Tet} \begin{bmatrix} m & m & m \\ k_2 & i_2 & 2 \end{bmatrix} \text{Tet} \begin{bmatrix} m & m & k_4 \\ k_3 & i_3 & 2 \end{bmatrix} \text{Tet} \begin{bmatrix} k_2 & k_3 & 2 \\ i_3 & i_2 & m \end{bmatrix} \Delta_{k_2} \Delta_{k_3}}{\theta(k_2, i_2, 2) \theta(k_3, i_3, 2) \theta(m, m, k_2) \theta(k_2, k_3, m) \theta(k_3, k_4, m)}$$

where

$$\mathcal{Q} = \frac{\lambda_{k_3}^{i_3 2}}{m} \left( \frac{-i_2 \text{Tet} \begin{bmatrix} k_2 & i_2 & i_2 \\ 2 & 2 & 2 \end{bmatrix}}{\theta(k_2, i_2, 2)} + \frac{i_3 \text{Tet} \begin{bmatrix} k_3 & i_3 & i_3 \\ 2 & 2 & 2 \end{bmatrix}}{\theta(k_3, i_3, 2)} \right). \quad (36)$$

We can write the Tets in this equation in terms of Wigner 6- $j$  symbols. At least one of the arguments of the resulting Wigner 6- $j$  symbols will be 1, and analytic

formulas for this case have been compiled (see, for example, Varshalovich [15]). Equation (21) then becomes

$$W_{[rst]i_2 \dots i_{n-2}}^{(n) k_2 \dots k_{n-2}} = -m^3 \mathcal{Q} \mathcal{R} \mathcal{S} \lambda_{k_2}^{i_2 2} \delta_{i_4}^{k_4} \dots \delta_{i_{n-2}}^{k_{n-2}} \quad (37)$$

where  $\mathcal{Q}$  is given in (36), and  $\mathcal{R}$  and  $\mathcal{S}$  are given by

$$\mathcal{R} = \left\{ \begin{array}{ccc} m/2 & k_2/2 & k_3/2 \\ 1 & i_3/2 & i_2/2 \end{array} \right\}_W \left\{ \begin{array}{ccc} m/2 & m/2 & k_2/2 \\ 1 & i_2/2 & m/2 \end{array} \right\}_W \left\{ \begin{array}{ccc} k_4/2 & m/2 & k_3/2 \\ 1 & i_3/2 & m/2 \end{array} \right\}_W \quad (38)$$

$$\mathcal{S} = \theta(m, m, 2) \sqrt{\frac{\theta(i_2, i_3, m) \theta(m, m, i_2) \theta(i_3, i_4, m)}{\theta(k_2, k_3, m) \theta(m, m, k_2) \theta(k_3, k_4, m)}}. \quad (39)$$

Note that we are using a  $W$  subscript to denote where we have used Wigner 6- $j$  symbols instead of the usual spin-network 6- $j$  symbols; see Ref. [7] for the exact correspondence between these sets of symbols.

Finally, we note that there are certain “selection rules” for finding the non-zero elements of  $W$  in this basis. The presence of a series of Kronecker deltas in (21) gives us the obvious selection rules that

$$k_4 = i_4, \quad k_5 = i_5, \quad \dots \quad k_{n-2} = i_{n-2}. \quad (40)$$

It is also evident from the spin diagram in (22) that for the 9- $j$  symbol in (21) to be non-zero, we must have

$$k_2 - i_2 = 0, \pm 2 \quad \text{and} \quad k_3 - i_3 = 0, \pm 2 \quad (41)$$

in order to satisfy the triangle inequalities. Finally, it can be shown that

$$\frac{a}{\theta(a, b, 2)} \text{Tet} \left[ \begin{array}{ccc} a & a & b \\ 2 & 2 & 2 \end{array} \right] = \begin{cases} (-1)^{a+1} \cdot \frac{a+2}{2} & b = a - 2 \\ -1 & b = a \\ (-1)^a \cdot \frac{a}{2} & b = a + 2 \\ 0 & \text{otherwise} \end{cases} \quad (42)$$

Hence, if  $k_2 = i_2$  and  $k_3 = i_3$ , the two terms in parentheses in (36) will be equal, and therefore cancel out, making the quantity  $\mathcal{Q}$  zero. We can then rewrite (41) as

$$\begin{aligned} k_2 - i_2 = 0, \pm 2, \quad k_3 - i_3 = 0, \pm 2, \quad \text{with} \\ k_2 - i_2 \text{ and } k_3 - i_3 \text{ are not both zero.} \end{aligned} \quad (43)$$

We conclude that for a given column of the  $W$  matrix (i.e. fixed  $k_2, k_3, \dots, k_{n-2}$ ), there will be at most eight non-zero elements:

$$\begin{aligned} i_2 = k_2 - 2 & \quad i_2 = k_2 - 2 & \quad i_2 = k_2 - 2 \\ i_3 = k_3 - 2 & \quad i_3 = k_3 & \quad i_3 = k_3 + 2 \\ \\ i_2 = k_2 & & \quad i_2 = k_2 \\ i_3 = k_3 - 2 & & \quad i_3 = k_3 + 2 \\ \\ i_2 = k_2 + 2 & \quad i_2 = k_2 + 2 & \quad i_2 = k_2 + 2 \\ i_3 = k_3 - 2 & \quad i_3 = k_3 & \quad i_3 = k_3 + 2 \end{aligned} \quad (44)$$

The quantities  $\mathcal{Q}$ ,  $\mathcal{R}$ , and  $\mathcal{S}$  are fairly simple to calculate for a given set of arguments. Finding the maximum product of all three, over all possible values

of  $k_2, k_3, k_4, i_2, i_3$ , and  $i_4$ , is a much more daunting task.<sup>4</sup> This task is further complicated by the fact that both the quantities  $\mathcal{Q}$  and  $\mathcal{R}$  have slightly different analytic forms for each of the eight entries in a given column — one form for  $k_2 - i_2 = 2$  and  $k_3 - i_3 = 2$ , one form for  $k_2 - i_2 = 2$  and  $k_3 - i_3 = 0$ , and so forth (see Varshalovich [15].)

Despite this difficulty, we can get an idea of the scaling properties of the absolute row and column sums by numerical analysis. By a happy coincidence, we do not even need to look at all of the rows and columns of the matrix — only a small subset of them. This is because (as mentioned above) the entries of the  $W$ -matrix are only dependent on the six values  $\{k_2, k_3, k_4, i_2, i_3, i_4\}$ ; all other pairs of corresponding indices must be equal, or the matrix entry will be zero. These facts imply that the  $W$ -matrix must be of block-diagonal form, and, more importantly, that each one of the blocks is identical. We see that we need only compute the absolute row and column sums for the (much smaller) block matrix, instead of the full  $W$ -matrix. This is still a non-trivial calculation, as the size of this matrix scales fairly quickly (for  $m = 10$  this matrix has already grown to  $891 \times 891$ ) but it does simplify the problem greatly.

Using this trick, combined with the selection rules in (40) and (43), the bounding quantity  $M$  (as defined above in section 3.3) may be calculated. Two methods were used. The first was the absolute row and column sum discussed previously. The second was MATLAB's internal `normest` function, which estimates the largest eigenvalue of a sparse matrix.<sup>5</sup> These results are shown in Figure 7. Each of these data sets is fitted to a power law relation. We see that for both of these data sets, we have an approximate relation  $M \propto m^3$ .

There is good reason to believe that this power dependence should tend towards  $m^3$  (exactly) as  $m \rightarrow \infty$ : if it does, then we have the relation

$$\begin{aligned} |\lambda_V| &\approx \sqrt{M \frac{n(n-1)(n-2)}{96}} \\ &\approx C\sqrt{m^3 n^3} \\ &= C(\text{total spin})^{3/2} \end{aligned} \tag{45}$$

where  $C$  is a proportionality constant. As noted in the previous section, this is the dependence expected from classical spatial geometry. While our data are not conclusive evidence of this relation, they are highly suggestive that this relation holds for a monochromatic vertex of any valence.

#### 4. CONCLUSIONS

We have seen some interesting consequences stemming from the discreteness of the angle operator. These results will be referred to as the *small angle* property, the *angular resolution* property, and the *angular distribution* property. We now wish to assign some scaling behavior to these predicted phenomena; in other words, on what length scales do we expect these phenomena to be observable?

<sup>4</sup> Note that, in a small mercy granted to us by equation (21), the entries of this form of the  $W$ -matrix depend only on these six intertwiner strands (and the edge colour  $m$ ) and not on the entire set.

<sup>5</sup> For the mathematically inclined reader, we note that the absolute row and column sums are known as the 1-norm and the  $\infty$ -norm of a given matrix, respectively; that which `normest` finds is the 2-norm.

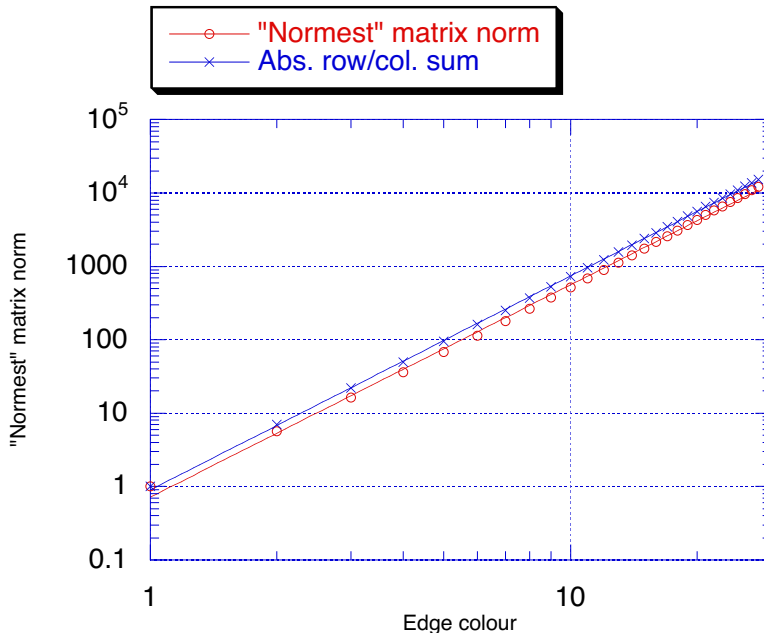


FIGURE 7. The eigenvalue limits found by the absolute row and column sums and by MATLAB’s internal `normest` function. The curve fits are for a power law relation. For the absolute row/column sum method, the best fit is  $M = 0.90432 \cdot x^{2.9126}$ ; for the `normest` method, it is  $M = 0.71884 \cdot x^{2.8921}$ .

The small angle property is the best-quantified of these three properties. We have the equation

$$\epsilon \geq \frac{4}{\sqrt{n+8}} \geq \frac{4}{\sqrt{s_T+8}}, \quad (46)$$

where  $s_T$  is the total surface flux. From our numerical studies of the volume operator, we also have the result that

$$V \propto L^3 \propto s_T^{3/2} \quad (47)$$

If we combine these results then we obtain the result that for large  $s_T$ , the minimum observable angle is related very simply to the length scale observed

$$\epsilon \propto L^{-1} \propto s_T^{-1/2} \quad (48)$$

where  $L$  is the characteristic length (in Planck units) defined by the volume or area. Thus, an accuracy of  $10^{-10}$  radians corresponds to spin fluxes of  $10^{20}$  and spin network vertices of  $L \sim 10^{-25}$ m. Moreover for large “background geometries” the primary limit is not from  $s_T$  but from  $(s_1 + s_2)$

$$\epsilon \propto (s_1 + s_2)^{-1/2}.$$

It is also possible to directly relate the minimum angle to the volume contribution of the spin network vertex. Using the same relations as above the dependence of

minimum angle and volume on the total spin flux implies the “minimum-angle volume bound” given by

$$\epsilon \frac{V^{1/3}}{\ell_P} \gtrsim 1. \quad (49)$$

One way to read this is that the smaller the minimum angle desired, the larger the volume contribution of the vertex, the larger the “quanta of volume.” Thus, this particular form of the angle operator suggests a very different description of our flat space. The effectively continuous spin network state would be a highly flocculent network of high valent vertices.

We note that this “bound” is based only on the considerations of the dependence of the spectra on the spin flux. It is not derived by the non-commuting properties of the operators. In addition to this bound, we expect that there would be a volume-angle uncertainty relation as there is in the case of the area operators [14].

In Section 2.3 we found results for the mean angular resolution associated with a vertex. The most important of these were the average spacing between expectation values for monochromatic vertices, given by

$$\delta \geq \frac{4\pi}{n^2 + 3n + 3}. \quad (50)$$

Combining these results with the result in Eq. (47) allows us to associate a scaling behavior with the mean angular separation and resolution. For large  $n$ , the angular separation scales as

$$\delta \propto n^{-2} \propto L^{-4}. \quad (51)$$

This scaling property of the angular resolution is somewhat striking, since it scales proportionally to such a high value of the total spin (i.e. inversely proportional to the fourth power of the length.)

We found that we could reproduce the classical angle distribution of  $\mathcal{P}(\theta) d\theta = \sin \theta d\theta$  under the condition that

$$1 \ll \{s_1, s_2\} \ll s_r.$$

In the absence of good analytical control on the precise behavior, it is not possible to determine the length scale to this condition. The importance of our angle distribution results is more clear in light of the small-angle results. The minimum angle observable depends on  $s_T$  if  $s_1, s_2 \approx s_r$ , but on  $s_1 + s_2$  if  $s_1, s_2 \ll s_r$ . To obtain the classical distribution the latter case holds and so the sum of the fluxes  $s_1$  and  $s_2$  must also be large. Thus, to approximate classical angles the total spin and the spin through surface patches  $S_1$  and  $S_2$  must be quite large.

Finally, in reflecting on these results it is important to keep in mind the nature of angle operator under consideration. Classically an angle is defined at the intersection of two lines - a point. In loop quantum gravity it is possible to define the angle at a single spin network vertex. As the above analysis shows, these “atoms of geometry” are small objects. It seems likely that to model familiar interactions which have “angle dependence” it will be necessary to average over many such vertices. If this in fact proves to be the case, then the above estimates must be modified.

**Acknowledgment.** *It is a pleasure to acknowledge the generous hospitality of Deep Springs College and summer research funds from Swarthmore College.*

## REFERENCES

- [1] C. Rovelli and L. Smolin, “Discreteness of area and volume in quantum gravity” *Nuc. Phys. B* **422** (1995) 593; [gr-qc/9411005](#).
- [2] S. Frittelli, L. Lehner, C. Rovelli, “The complete spectrum of the area from recoupling theory in loop quantum gravity” *Class. Quant. Grav.* **13** (1996) 2921-2932; [gr-qc/9608043](#).
- [3] A. Ashtekar and J. Lewandowski, “Quantum theory of geometry I: Area operators” *Class. Quant. Grav.* **14** (1997) A43-A53; [gr-qc/9602046](#).
- [4] A. Ashtekar and J. Lewandowski, “Quantum theory of geometry II: Volume operators” *Adv. Theor. Math. Phys.* **1** (1998) 388; [gr-qc/9711031](#).
- [5] R. DePietri and C. Rovelli, “Geometry eigenvalues and the scalar product from recoupling theory in loop quantum gravity” *Phys. Rev. D* **54** (1996) 2664-2690; [gr-qc/9602023](#).
- [6] S. Major, “Operators for Quantized Directions” *Class. Quant. Grav.* **16** (1999) 3859; [gr-qc/9905019](#).
- [7] M. Seifert. “Angle and Volume Studies in Quantized Space” *BA Thesis* Swarthmore College 2001 [gr-qc/0108047](#).
- [8] S. Major, “New Operators for Spin Net Gravity: Definitions and Consequences” [gr-qc/0101032](#).
- [9] R. Penrose, “Angular momentum: An approach to combinatorial spacetime” in *Quantum Theory and Beyond* edited by T. Bastin (Cambridge University Press, Cambridge, 1971); “Combinatorial Quantum Theory and Quantized Directions” in *Advances in Twistor Theory*, Research Notes in Mathematics 37, edited by L. P. Hughston and R. S. Ward (Pitman, San Francisco, 1979) pp. 301-307; in *Combinatorial Mathematics and its Application* edited by D. J. A. Welsh (Academic Press, London, 1971); “Theory of Quantized Directions,” unpublished notes.
- [10] J. P. Moussouris, “Quantum models as spacetime based on recoupling theory” *DPhil Thesis* Oxford University 1983.
- [11] N. Grot and C. Rovelli. “Moduli-space structure of knots with intersections” *J. Math. Phys.* **37** (1996) 3014.
- [12] N. Grot, “Topics in Loop Quantum Gravity” *MS Thesis* University of Pittsburgh 1998.
- [13] R. De Pietri. “Spin Networks and Recoupling in Loop Quantum Gravity” *Nucl. Phys. Proc. Suppl.* **57** (1997) 251-254.
- [14] A. Ashtekar, A. Corichi, and J. A. Zapata, “Quantum Geometry III: Non-commutativity of Riemannian Structures” *Class. Quant. Grav.* **15** (1998) 2955-2972; [gr-qc/9806041](#).
- [15] D.A. Varshalovich, A.N. Moskalev, and V.K. Khersonskii, *Quantum Theory of Angular Momentum* (World Scientific, Teaneck, NJ, 1988).

MAJOR: DEPARTMENT OF PHYSICS, HAMILTON COLLEGE, CLINTON NY 13323 USA, SEIFERT: DEPARTMENT OF PHYSICS AND ASTRONOMY, SWARTHMORE COLLEGE, SWARTHMORE PA 19081 USA

*E-mail address:* Major: [smajor@hamilton.edu](mailto:smajor@hamilton.edu), Seifert: [seifert@scs.swarthmore.edu](mailto:seifert@scs.swarthmore.edu)